Polytopal Rearrangement of [Ni(acac)$_2$(py)]: A New Square Pyramid⇌Trigonal Bipyramid Twist Mechanism

Claude Daul,[b] Svetozar Niketic,*[a, b] Cédrick Rauzy,[b] and Carl-Wilhelm Schläpfer[b]

Keywords: density functional calculations · fluxionality · molecular modeling · N ligands · nickel · O ligands · pentacoordination

Abstract: The interconversion mechanisms between three idealized polytopal forms (a square pyramid and two trigonal bipyramids) of [M(bidentate)$_2$(unidentate)] were investigated by an original combination of molecular mechanics (MM) and density functional theory (DFT) approaches. MM was used to model the mechanistic rearrangement path, and DFT to study selected points along this path. The test case was a five-coordinate [Ni(acac)$_2$-(py)] species. In the case of [Ni(acac)$_2$-(py)] it was confirmed (both by MM and by DFT) that the three polytopal forms do indeed represent shallow local minima, of which the square pyramid (SQP) is more stable than the other two. Small energy barriers that separate the three minima prevent spontaneous rearrangement among the polytopal forms in geometry-optimization simulations. The driving force for MM simulation of the polytopal rearrangements was supplied through the L-M-L angle bending terms. MM results for relative energies and geometries are fully supported by DFT. Finally, the implication of the present results to explain some racemization mechanisms of octahedral complexes (namely, the intramolecular bond rupture of tris(chelate) species, and intermolecular dissociation of bis(bidentate) species) is briefly discussed.

Introduction

Polytopal rearrangements of pentacoordinate structures have been much studied in the past. Most detailed mechanistic descriptions of intramolecular rearrangements are to be found among the papers of Muetterties et al.[1] as well as others.[2] More recently, a full ab initio molecular dynamics study of the polytopal rearrangement was described for the PF$_5$ molecule.[3]

Coordination number five in metal complexes has been systematically investigated by Kepert[4] who treated, among other structural types, the [M(bidentate)$_2$(unidentate)] species.[5] However, Kepert did not comment on the possibility for the existence of a trigonal bipyramid (TBP) with a unidentate ligand in the axial position, and possible mechanisms for the interconversion between the square pyramid

(SQP) and two distinct TBP structures (with unidentate in the axial as well as in the equatorial position of a TBP). In the following discussion we shall label the last two possibilities as TBP$_{ax}$ and TBP$_{eq}$, respectively (see Figure 1).

It is reasonable to assume that a SQP⇌TBP$_{eq}$ interconversion proceeds by the Berry twist mechanism.[6] However, for the SQP⇌TBP$_{ax}$ interconversion, an equally simple mechanistic path could not be defined. Moreover, it seems that it is not possible to convert SQP into a TBP$_{ax}$ structure, and at the same time to preserve the bite angles of two bidentate ligands, without substantial deformations of other valence angles on the metal center.[7]

In this work we use the molecular mechanics (MM) approach to study the interconversion paths between SQP, TBP$_{ax}$, and TBP$_{eq}$ structures for a [M(bidentate)$_2$(unidentate)] type of compound exemplified by the [Ni(acac)$_2$(py)] complex. We succeeded at simulating the transformation of all three structures into each other. In addition, we propose an unrecognized mechanism, up to this time, for accessing the TBP$_{ax}$ structure from the other two, which involves the least possible distortion of valence angles on the central atom. MM results are complemented with DFT calculations on selected intermediate configurations along each of the three interconversion paths, as well as with full geometry optimization of SQP, TBP$_{ax}$, and TBP$_{eq}$ structures.

[a] Prof. S. Niketic
Roche Research Fellow (2001–2002)
Department of Chemistry, University of Belgrade
Studentski Trg 16, Box 158, 11001 Belgrade
Serbia & Montenegro (Yugoslavia)

[b] Prof. C. Daul, Prof. S. Niketic, C. Rauzy, Prof. C.-W. Schläpfer
Département de Chimie
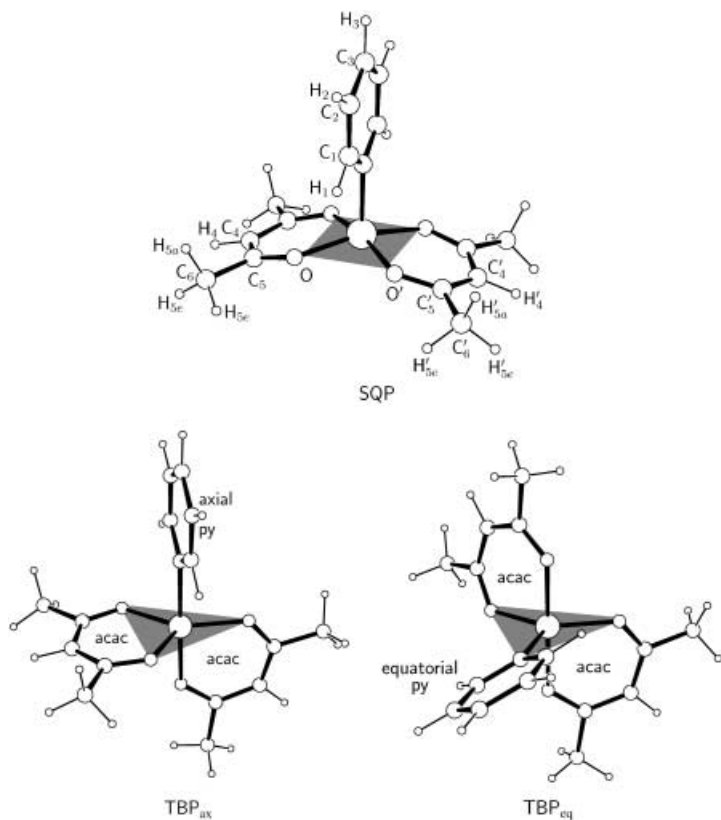Université de Fribourg-Pérolles
1700 Fribourg, (Switzerland)

Figure 1. Three polytopal forms of [Ni(acac)$_2$(py)]: square pyramid (SQP) with the atom numbering scheme, trigonal bipyramid with axial unidentate py (TBP$_{ax}$), and trigonal bipyramid with equatorial unidentate py (TBP$_{eq}$). The structures fully depict optimized geometries by the DFT method.

Computational Methods

MM calculations: All MM calculations described in this study were performed with the CFF program package[8] with essentially the same protocols (unless otherwise noted); these were recently used by us in the studies of other coordination chemistry structures.[9]

The aim of MM investigations carried out in this work was not to optimize a force field on the [Ni(acac)$_2$(py)] structure. Therefore, we used previously developed MM parameters[9] with a few necessary additions required for structures that contain pyridine (extrapolated from the widely used force fields AMBER[10] or SYBIL[11]), as well as with additions necessary for acac chelates, drawn from our previous work.[12]

In order to be able to compare the relative energies for all three forms of the [Ni(acac)$_2$(py)] structure, namely SQP, TBP$_{ax}$, and TBP$_{eq}$ (Figure 1), we introduced the "double-well" functions for the treatment of angle-bending on the Ni atom, as shown in Equation (1) below,

$$E(\phi) = h\left[1 - \frac{(\phi - A - B)^2)}{B^2}\right]^2 \tag{1}$$

in which parameters A and B define positions of the minima, and parameter h the barrier between the minima (ϕ is used to denote any L-M-L angle throughout this paper). A typical example of this "double-well" function, shown in Figure 2, exhibits minima at 90° and 120°. This function is applied, for example, in describing the bending of a particular N-Ni-O angle with an equilibrium value of 90° for SQP or 120° for TBP$_{eq}$ configuration.

DFT calculations: The DFT calculations were performed by using the Amsterdam Density Functional (ADF) program package (Release
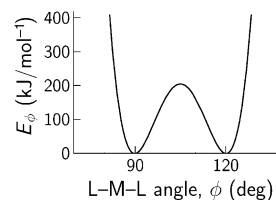

Figure 2. Double-well function with minima at 90° and 120°. With $h = 500$, it was possible to approximate the curvature in the vicinity of the minima comparable to that obtained with normal harmonic functions for L-M-L angle bending.

2000.02).[13] We used the spin-unrestricted formalism with an overall charge of zero for the species, and a difference of two between spin alpha and spin beta configuration. Both the local density approximation (LDA) and the generalized gradient approximation (GGA) for exchange-correlation functionals were used, but for all plot and data displayed in this article, we refer to the GGA approximation. The LDA was applied with the α functional for exchange ($\alpha = 0.7$),[14] and the Vosko, Wilk, and Nusair functional for correlation.[15] The GGA was applied by using the Becke 88[16] exchange and the Perdew 86[17] correlation (BP). The frozen-core approximation for the inner core electrons was used for all non-hydrogen atoms. The orbitals up to 2p for nickel and 1s for nitrogen, oxygen, and carbon were kept frozen. The valence shells were described by a triple-ζ STO (slater-type orbital) set, plus one polarization function.

Geometry optimizations were performed by using the Broyden–Fletcher/Goldfarb–Shanno algorithm to update the Hessian matrix.[18] The energy convergence criteria for ADF was 10^{-6} au, and the numerical integration used was a default.

Results and Discussion

MM results: MM results for the SQP, TBP$_{ax}$, and TBP$_{eq}$ forms of [Ni(acac)$_2$(py)] are shown in Table 1. They show that there are no significant differences in strain energy between the three structures. Therefore, it was not practical to simulate the intramolecular rearrangement within this force field. To provide for a driving force, which would bring about the interconversion, we attempted to modify the L-M-L angle bending potential by decreasing the barrier, h, between the two minima in the double-well functions. Eventually, the simulation of interconversions was accomplished by completely removing the barrier h, that is, by using functions with single minima adjusted to desired values.

Therefore, MM calculations were performed starting from the previously optimized regular structures, by supplying in each case, the target values of L-M-L angles for the desired form (SQP, TBP$_{eq}$, or TBP$_{ax}$), and by allowing for the full relaxation of all internal coordinates.

Table 1. MM total energies and energy contributions [kJ mol^{-1}] for the equilibrium structures of SQP, TBP$_{eq}$, and TBP$_{ax}$ forms of [Ni(acac)$_2$-(py)]. The difference between E(total), and the sum of the terms is due to the Coulomb contribution.

	SQP	TBP$_{eq}$	TBP$_{ax}$
Total energy	−102.72	−95.27	−97.46
E(bonds)	3.66	4.42	5.95
E(angles)	8.32	28.58	28.00
E(torsions)	0.43	2.78	1.19
E(nonbonded)	−12.22	−12.23	−11.12

SQP⇌TBP$_{eq}$ rearrangement: The SQP⇌TBP$_{eq}$ rearrangement proceeds in a straightforward way. Starting from the "ideal" SQP form (with the metal in the basal plane of four oxygen ligators), a simultaneous symmetric angular-bending of two *trans* oxygens of SQP (N-Ni-O angle: 90°→120°) produces the TBP$_{eq}$. This interconversion path is similar to the corresponding segment of the well known Berry twist mechanism.[6]

However, if we start from the SQP form of [Ni(acac)$_2$-(py)] with the Ni atom displaced from the basal plane towards the pyridine apex (which is more likely to be the equilibrium configuration of this compound), the rearrangement reduces essentially to the opening of one of the *trans* O-Ni-O angles to 180°.

Both paths are relatively short (in the configurational space), which is consistent with the small energy difference between SQP and TBP$_{eq}$, and are easily followed in a direction determined by the choice of the target values for L-M-L angles. Ligator atom labeling convention and the choice of target L-M-L angles is shown in Table 2. Figure 3 depicts the changes of all angles around the central metal atom in the course of the SQP⇌TBP$_{eq}$ rearrangement.

Figure 3. A sketch showing the changes in L-M-L angles in the course of the SQP⇌TBP$_{eq}$ rearrangement. The curves were obtained by a polynomial fit to the angle values at each geometry-optimization step. Angles ϕ are defined in Table 2.

Figure 4. A sketch of the SQP⇌TBP$_{ax}$ interconversion path. It shows that both acac rings undergo specific concerted angular-distortions at the Ni atom, and maintain approximate bilateral symmetry if the chelate rings are neglected (see text for further description of the interconversion mechanism).

Table 2. Target L-M-L angles for the SQP⇌TBP$_{eq}$ rearrangement.

Angle	Description	Ideal SQP value	TBP$_{eq}$ value	DFT SQP	DFT TBP$_{eq}$
ϕ_1	O$_A$-Ni-O$_{A'}$	90	90	92.484	91.148
ϕ_2	O$_A$-Ni-O$_B$	90	90	85.680	87.510
ϕ_3	O$_A$-Ni-O$_{B'}$	180	120	165.615	138.516
ϕ_4	O$_A$-Ni-N	90	120	97.340	109.257
ϕ_5	O$_{A'}$-Ni-O$_B$	180	180	165.615	175.174
ϕ_6	O$_{A'}$-Ni-O$_{B'}$	90	90	85.680	87.410
ϕ_7	O$_{A'}$-Ni-N	90	90	97.340	93.127
ϕ_8	O$_B$-Ni-O$_{B'}$	90	90	92.484	90.525
ϕ_9	O$_B$-Ni-N	90	90	97.340	91.692
ϕ_{10}	O$_{B'}$-Ni-N	90	120	97.340	112.220

SQP⇌TBP$_{ax}$ rearrangement: The SQP⇌TBP$_{ax}$ rearrangement was much more difficult to attain. It proceeds through the following intricate mechanism (see Figure 4), which to our knowledge, has not been described before now. Ligand atom labeling and the values of target L-M-L angles are shown in Table 3, and the changes of all angles around the central metal atom is shown in Figure 5.

One of the oxygen atoms of the basal plane in SQP undergoes an angular bending displacement (N-Ni-O angle ϕ_{10}: 90°→180°) in the plane that contains nickel, nitrogen, and oxygen atoms that was initially *trans* to it. Simultaneously, two other oxygen atoms (*trans* to each other in the initial SQP structure) start to spin around their M-L axes in a remarkably concerted way, following a semi-spiral path. Their movement causes two of the O-Ni-O angles (ϕ_6 and
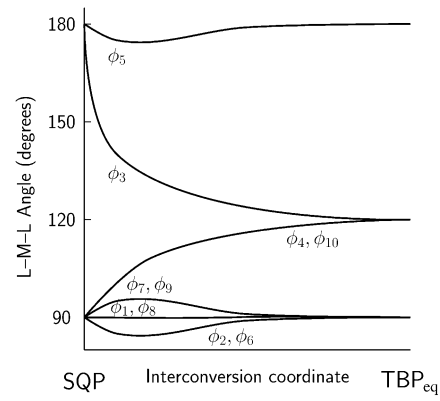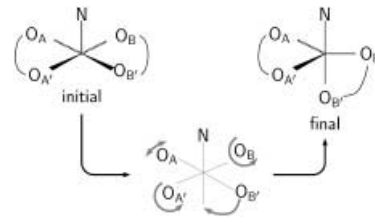
Table 3. Target L-M-L angles for the SQP⇌TBP$_{ax}$ rearrangement.

Angle	Description	Ideal SQP value	TBP$_{ax}$ value	DFT SQP	DFT TBP$_{ax}$
ϕ_1	O$_A$-Ni-O$_{A'}$	90	90	92.437	95.811
$\phi2$	O$_A$-Ni-O$_B$	90	135	85.711	130.009
$\phi3$	O$_A$-Ni-O$_{B'}$	180	90	165.407	92.017
$\phi4$	O$_A$-Ni-N	90	90	97.297	89.676
$\phi5$	O$_{A'}$-Ni-O$_B$	180	135	165.407	130.044
$\phi6$	O$_{A'}$-Ni-O$_{B'}$	90	90	85.711	90.713
$\phi7$	O$_{A'}$-Ni-N	90	90	97.297	89.193
$\phi8$	O$_B$-Ni-O$_{B'}$	90	90	92.437	90.935
$\phi9$	O$_B$-Ni-N	90	90	97.297	87.916
$\phi10$	O$_{B'}$-Ni-N	90	180	97.297	178.306

ϕ_8), as well as the O-Ni-N angle, ϕ_4, to close first slightly below 90°, and then to open up back to 90°. The O-Ni-N angles (ϕ_7 and ϕ_9) behave in exactly the opposite way: they open first and then close back to 90°.
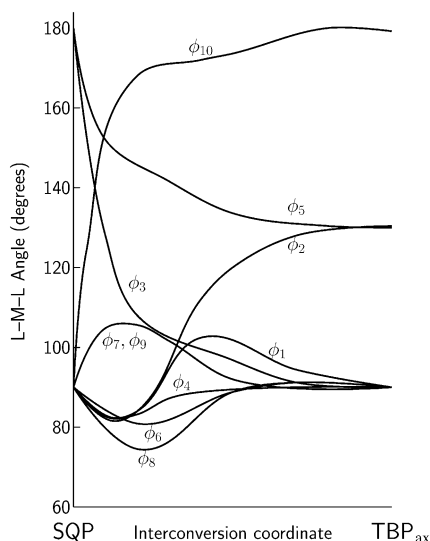
Figure 5. Changes in L-M-L angles in the course of the SQP⇌TBP$_{ax}$ rearrangement. The curves were obtained by a polynomial fit to the angle values at each geometry-optimization step. Angles ϕ are defined in Table 3.

The point corresponding approximately to the simultaneous extrema of L-M-L angles ϕ_4, ϕ_6, ϕ_7, ϕ_8, and ϕ_9 (cf. the notation defined in Table 3) represents the transition state for the SQP⇌TBP$_{ax}$ interconversion.

From the correlations between the pairs of ϕ angles in the SQP⇌TBP$_{ax}$ rearrangement it may be concluded that this mechanism is essentially a two-step process.

There are two subtle variants of the foregoing mechanism. If we allow the chelate angles to open easily, so that the O-Ni-O angle of the equatorial acac could approach a value of 120° (corresponding to a "regular" TBP value), then the above mentioned concerted movement of the oxygen atoms (*trans* in SQP) is preserved. However, if we constrain the chelate angles to approximtely 90°, the movement of the pair of oxygen atoms become decoupled (oxygen belonging to the acac ring of the equatorial plane becomes much less mobile), and the whole mechanism loses some "symmetry". It is most probable that the true rearrangement path exists between these two extrema, and therefore retain a clearly discernible pattern in the concurrent movement of oxygen ligators, as described above.

TBP$_{ax}$⇌TBP$_{eq}$ rearrangement: The interconversion between two TBP forms of [M(bidentate)$_2$(unidentate)] structures also seems to follow an intricate mechanism (see Table 4 and Figure 6). It is characterized by a concerted movement of both chelate rings. In the present simulation, driven solely by the choice of the target L-M-L angles, the two forms rearranged into each other by a mechanism that *did not* involve a passage through the SQP geometry.

DFT results: Initially we attempted to use DFT to calculate the three paths, defined above, by the linear transit procedure (calculation in which a motion of one atom is defined, in general, by changing the value of one angle, and performing a full optimization of the molecule, except for the fixed

Table 4. Target L-M-L angles for the TBP^{ax}⇌TBP$_{eq}$ rearrangement.

Angle	Description	TBP^{ax} value	TBP^{eq} value	DFT TBP^{ax}	DFT TBP^{eq}
ϕ1	O$_A$-Ni-O$_{A'}$	90	90	91.647	92.412
ϕ2	O$_A$-Ni-O$_B$	90	120	91.894	140.676
o3	O$_A$-Ni-O$_{B'}$	90	90	90.358	88.197
ϕ4	O$_A$-Ni-N	180	120	177.678	104.899
ϕ5	O$_A$-Ni-O$_B$	135	90	119.500	87.841
ϕ6	O$_A$-Ni-O$_{B'}$	135	180	144.195	178.745
ϕ7	O$_A$-Ni-N	90	90	88.978	85.574
ϕ8	O$_B$-Ni-O$_{B'}$	90	90	96.143	92.384
ϕ9	O$_B$-Ni-N	90	120	90.389	114.424
ϕ10	O$_{B'}$-Ni-N	90	90	87.593	89.208
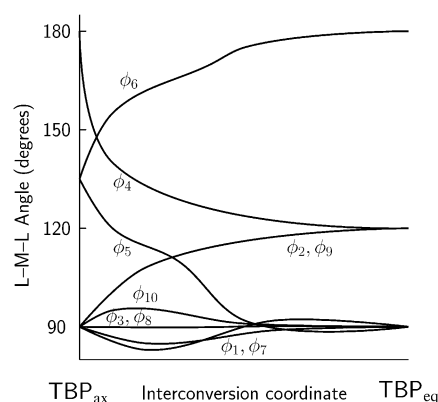
Figure 6. A sketch showing the changes in L-M-L angles in the course of the TBP$_{ax}$⇌TBP$_{eq}$ rearrangement. The curves were obtained by a polynomial fit to the angle values at each geometry-optimization step. Angles (ϕ) are defined in Table 4.

angle value at each point of the displacement path). However, this approach turned out not to be feasible, because the transitions are not easily defined due to the pentacoordination of nickel. In addition, the linear transit approach is very time consuming due to the lack of symmetry of most of the intermediate geometries along the path. Finally, difficulties in reaching the convergence criteria for the intermediate conformations should be beared in mind.

This prompted us to use the path defined by MM calculation to perform the single-point DFT calculations, and to perform geometry optimization and frequency calculations on the terminal geometries only.

However, before doing any simulation on the path, we took interest in the pyridine rotation energy on the SQP form. For this particular displacement, which is easy to define (depending only on one dihedral angle), we adopted the linear transit approach.

Pyridine rotation simulation on the SQP: The purpose of the calculations was to see if pyridine was able to rotate freely about the metal–nitrogen bond. We made a full geom-

etry optimization on the SQP form to get the most stable angle between the Ni–N bond and the Ni–O bonds. The full optimization showed that the pyridine plane is perpendicular to the C_4-Ni-C'_4 axis (cf. Figure 1). To examine the energy profile of pyridine rotation, we did a linear transit calculation by changing the value of the dihedral angle C_4-N-Ni-C_1 from 0 to 90°. The full rotational energy profile is displayed in Figure 7.
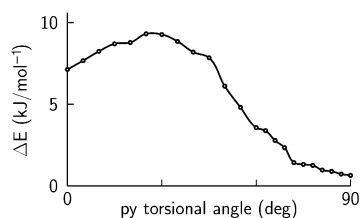

Figure 7. DFT energy profile for the rotation of pyridine about the Ni–N bond in the SQP structure optimized by DFT. Reference torsional angle is C_4-Ni-N-C_1 (see the numbering scheme in Figure 1) The relative energy scale is in kJ mol^{-1}.

We can see that the maximum of the curve is at about 30 degrees, which could be due to the steric repulsion between the oxygen and the pyridine hydrogen. We can also observe that the rotation of the pyridine costs less than 10 kJ mol^{-1} for one quarter of a rotation, and the difference between the two limiting position are less than 7 kJ mol^{-1}. Therefore, we conclude that the pyridine can rotate freely, and that a change in the value of a dihedral angle along Ni–N is not really expensive in energy.

Geometry optimization: Next we attempted to verify our hypothesis that the three structures SQP, TBP$_{eq}$, and TBP$_{ax}$ are three (local) minima on the potential surface. For this, we took the geometries corresponding to the final structures of each path (that is, two structures per path) defined by MM calculations, and we performed a full optimization calculation on each of them to see if any of them could reach the other corresponding terminal geometry. Since it was never the case, the DFT results confirmed our hypothesis that the SQP, TBP$_{eq}$, and TBP$_{ax}$ are indeed three minima. The DFT results are shown in Figure 8 in which double arrows are used to emphasize that each interconversion

path was investigated in both directions. The number at the end of each path represents the relative energy (in kJ mol^{-1}) of the minimum with respect to the lowest energy SQP structure, which is reached starting from the structure indicated on the same side of the triangle in this scheme. The difference between the pairs of numbers that correspond to any of the three structures is due to the cut-off during geometry optimization procedure, and the fact that the energy surface is almost flat. To obtain the true convergence (the same or closer energy value for the same structure) we should extend the integration grid, but for geometry optimization this would be extremely time consuming. Nevertheless, cartesian coordinates for each pair of DFT optimized structures are very close to each other. The values of L-M-L angles for both structures of each pair are given in Tables 2, 3, and 4.

Single-point calculation: Next we modeled the energy surface of each path between the three minima in three sets of calculations. The MM calculations for each path afforded a succession of 100 to 200 sets of coordinates (points on the path for which we have sets of coordinates). To do DFT calculations on all the intermediate geometries is neither feasible nor necessary. We have instead carefully selected about ten points for each interconversion path. The chosen points are assumed to fairly continuously represent the key intermediate structures, in the sense that their succession provides a good description of the interconversion mechanism. Since the geometry optimization in MM does not generally proceed in a smooth way (for example, there are many moves in "false" directions in the vicinity of strong curvatures on the potential energy surface) we thus had a possibility to discard a number of points along the MM path, which corresponded to the intermediate structures with small energy gradients.

The results obtained for the three paths (SQP⇌TBP$_{ax}$, SQP⇌TBP$_{eq}$ and TBP$_{ax}$⇌TBP$_{eq}$) are presented in Figure 9. To ascertain that maxima along these paths do indeed origi-

Figure 9. DFT energy profiles for the interconversion between SQP, TBP$_{ax}$, and TBP$_{eq}$ configurations of [Ni(acac)$_2$(py)]. The TBP$_{ax}$⇌TBP$_{eq}$ (top), SQP⇌TBP$_{ax}$ (middle), and SQP⇌TBP$_{eq}$ path (bottom) were obtained with the optimization of bond lengths. The vertical axes represent relative energy (in kJ mol^{-1}) with arbitrary offset.
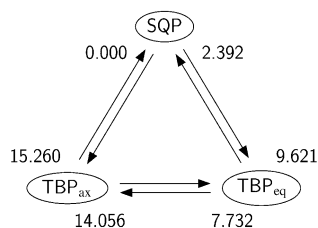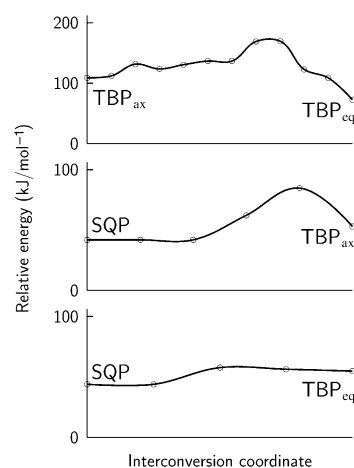

Figure 8. Energies (in kJ mol^{-1}) of fully optimized structures by DFT in relation to the interconversion path through which they have been obtained. Two values for each of the three polytopal forms refer to the structures obtained from each of the other two forms (on the same edge of the triangle).

nate from polytopal rearrangement, we also relaxed the restriction of a single-point DFT calculation by allowing for geometry optimization of all internals except L-M-L angles. In two cases (TBP$_{ax}$⇌TBP$_{eq}$ and SQP⇌TBP$_{ax}$ paths) lowering of barriers (Figure 9) was obtained, the difference being solely due to the adjustment of the Ni–N bond. All other geometry parameters remained essentially the same as in single-point DFT calculations.

Frequencies: The normal modes and vibrational frequencies were evaluated at the computed C_{2v} equilibrium geometry for the SQP and asymmetrical TBP forms.

Under C_{2v} symmetry the 114 fundamental vibrational modes of the SQP [Ni(acac)$_2$(py)] span the following irreducible representations, as shown in Equation (2).

$$33A_1 + 23A_2 + 28B_1 + 30B_2 \qquad (2)$$

The DFT computed infra-red spectrum of the SQP form appears essentially as a superposition of the features (observed or calculated by others) in acetylacetonato chelates and pyridine-N complexes. The assignment is therefore more easy than for the calculated spectra of TBP forms. Due to the lack of symmetry, the latter exhibit a considerable mixing of acac and py vibrations. Complete tables of calculated vibrational frequencies (12 pages), and a discussion of their assignment relative to published data are available from authors upon request.

Conclusion

In this work we investigated possible interconversion mechanisms between three idealized polytopal forms of [M(bidentate)$_2$(unidentate)] pentacoordinate structure: SQP, TBP$_{eq}$, and TBP$_{ax}$. The test case was a five-coordinate [Ni(acac)$_2$(py)] species, which is assumed to be an intermediate in the formation of the corresponding octahedral bis(pyridine) complex. This complex was experimentally investigated in the course of the study on [Ni(tmhd)$_2$(py)$_x$] (x=1,2) structures (tmhd=2,2,6,6-tetramethyl-3,5-heptanedionate).[19] The general method was an original QM/MM approach in which the MM and QM methods were applied in a consecutive way. In other words, MM was used to model the mechanistic rearrangement path, and QM to study selected points along this path. In this way, with MM we were able to propose a possible rearrangement mechanism circumventing the time-consuming QM geometry optimizations and linear-transit calculations. Subsequently, single-point QM calculations were performed on a carefully chosen sequence of structures, which defined the MM rearrangement model.

In the case of [Ni(acac)$_2$(py)] it was shown that the three polytopal forms (SQP, TBP$_{eq}$, and TBP$_{ax}$) do represent shallow local minima on the potential-energy surface. The SQP structure is the global minimum, which is more clearly defined than the other two. Shallow local minima are separated from each other by low-energy barriers, that do permit easy interconversion, but prevent spontaneous transformation among SQP, TBP$_{eq}$, and TBP$_{ax}$ forms in our geometry-

optimization simulation experiments. In MM calculations the polytopal rearrangement could be achieved only by supplying a specific driving force to the bending of L-M-L angles. DFT calculations support the assumption of three minima, in that, the minima are sufficiently shallow to impede exact convergence among the points close to the minima. In a previous ab initio (DFT) study of the Berry pseudo-rotation of PF$_5$ from this laboratory[3] a low activation energy and a rapid interconversion were predicted for this compound, however; the compound is quite different from the present nickel complex (apart from its coordination number).

The results of this investigation may provide a rationale for some racemization mechanisms of six-coordinate chelate complexes that involve SQP or TBP intermediates.[20] For example, both racemization and isomerization of chiral *cis*-bis(bidentate) octahedral species may proceed by a dissociative (S_N1) process via SQP or TBP intermediates,[20] which are shown in this work to be readily interconvertible. Similarly, the facility of the bond rupture racemization mechanism of tris(bidentate) species, proposed already by Werner[21] to be intramolecular, appears to be feasible according to the present investigation; this is mostly due to the ease of interconversion between SQP or TBP intermediates, as has been hypothesized by Muetterties[22] some time ago.

Finally, please note, we do not claim that [Ni(acac)$_2$(py)] species does exist in *three distinct* polytopal forms (SQP, TBP$_{eq}$, and TBP$_{ax}$). They merely reflect the initial conceptual confines of this study,[23] which is based on the fact that SQP and TBP geometries were indeed established in numerous previous studies of coordination number five in general, and that such taxonomy also offers a convenient framework for the analysis of highly fluxional structures, as may presumably be the case with [Ni(acac)$_2$(py)]. The three minima modeled by MM are the consequence of the force field employed in this work, which is not optimized on [Ni(acac)$_2$(py)] for obvious reasons, and which articulates the above mentioned conceptual framework through the choice of parameters in metal-ligand angle-bending functions. DFT modeling, which is less dependent on the kind of premise initially adopted in this work, still corroborates the concept of three minima, and even if any of our particularly shallow minima turn out to be a "transient minimum", the main conclusions and consequences of this research would remain valid.

[1] a) E. L. Muetterties, *J. Am. Chem. Soc.* **1969**, *91*, 1636–1643; b) E. L. Muetterties, *J. Am. Chem. Soc.* **1969**, *91*, 4115–4122; c) P.

Meakin, E. L. Muetterties, J. P. Jesson, *J. Am. Chem. Soc.* **1972**, *94*, 5271–5285; d) P. Meakin, E. L. Muetterties, F. N. Tebbe, J. P. Jesson, *J. Am. Chem. Soc.* **1971**, *93*, 4701–4709.

[2] a) P. C. Lauterbur, F. Ramirez, *J. Am. Chem. Soc.* **1968**, *90*, 6722–6726; b) J. D. Dunitz, V. Prelog, *Angew. Chem.* **1968**, *80*, 700–701; *Angew. Chem. Int. Ed. Engl.* **1968**, *7*, 725–726; c) J. Demuynck, A. Strich, A. Veillard, *Nouv. J. Chim.* **1977**, *1*, 217–228; d) K. Mislow, *Pure Appl. Chem.* **1971**, *43*, 549–562.

[3] C. Daul, M. Frioud, O. Schafer, A. Selloni, *Chem. Phys. Lett.* **1996**, *262*, 74–79.

[4] a) D. L. Kepert, *Inorg. Chem.* **1973**, *12*, 1938–1942; b) D. L. Kepert in *Comprehensive Coordination Chemistry, Vol. 1* (Eds.: G. Wilkinson, R. D. Gillard, J. A. McCleverty), Pergamon, London, **1987**, pp. 31–107.

[5] D. L. Kepert, *Inorg. Chem.* **1973**, *12*, 1942–1944.

[6] R. S. Berry, *J. Chem. Phys.* **1969**, *50-51*, 923–933. It should be noted that Berry originally proposed a mechanism for the interconversion between two TBP forms via an SQP transition state; therefore, the SQP⇌TBP_{eq} rearrangement is effectively only "one half" of a Berry twist.

[7] A. Lipkovski, personal communication to SRN (**2001**).

[8] S. R. Niketic, Kj. Rasmussen, *The Consistent Force Field: Lecture Notes in Chemistry, Vol. 3*, Springer, New York, **1977**.

[9] a) S. Grubisic, M. Gruden, S. R. Niketic, N. Sakagami-Yoshida, S. Kaizaki, *J. Mol. Struct.* **2002**, *609*, 1–9; b) S. Grubisic, M. Gruden-Pavlovic, S. R. Niketic, N. Sakagami-Yoshida, S. Kaizaki, *Transition Met. Chem.* **2003**, *28*, 37–42; c) M. Gruden, S. Grubisic, S. R. Niketic, A. G. Coutsolelos, *J. Mol. Struct.* **2001**, *595*, 209–224.

[10] W. D. Cornell, P. Cieplak, C. I. Bayly, I. R. Gould, K. M. Merz Jr., D. M. Ferguson, D. C. Spellmeyer, T. Fox, J. W. Caldwell, P. A. Kollman, *J. Am. Chem. Soc.* **1995**, *117*, 5179–5197.

[11] M. Clark, R. D. Cramer III, N. van Opdenbosch, *J. Comput. Chem.* **1989**, *10*, 982–1012.

[12] S. R. Niketic, unpublished MM studies of trigonal tris(bidentate) oxalato, malonato, and acetylacetonato complexes.

[13] a) *Amsterdam Density Functional (ADF) Program System*, Scientific Computing and Modeling NV, Theoretical Chemistry, Vrije Universiteit, Amsterdam, **2002**; b) E. J. Baerends, D. E. Ellis, P. Ros, *Chem. Phys.* **1973**, *2*, 41–51; c) P. M. Boerrigter, G. Te Velde, E. J. Baerends, *Int. J. Quantum Chem.* **1988**, *33*, 87–113; d) G. Te Velde, E. J. Baerends, *J. Comput. Phys.* **1992**, *99*, 84–98; e) C. Fonseca Guerra, O. Visser, J. G. Snijders, G. Te Velde, E. J. Baerends, in *Methods and Techniques in Computational Chemistry, Chap. 8* (Eds.: E. Clementi, C. Corongiu), STEF, Cagliari, **1995**, p. 305.

[14] J. C. Slater, *Quantum Theory of Molecules and Solids, Vol. 4 (Self Consistent Field for Molecules and Solids)*, McGraw-Hill, New York, **1974**.

[15] S. H. Vosko, L. Wilk, M. Nusair, *Can. J. Phys.* **1980**, *58*, 1200–1211.

[16] A. D. Becke, *Phys. Rev.* **1988**, *A38*, 3098–3100.

[17] J. P. Perdew, *Phys. Rev.* **1986**, *B33*, 8822–8824.

[18] W. H. Press, B. P. Flannery, S. A. Teukolsky, W. T. Vetterling, *Numerical Recipes*, 2nd ed., Cambridge University Press, Cambridge, **1992**.

[19] F. Emmenegger, C. W. Schlaepfer, H. Stoeckli-Evans, M. Piccand, H. Piekarski, *Inorg. Chem.* **2001**, *40*, 3884–3888.

[20] N. Serpone, D. G. Bickley, *Prog. Inorg. Chem.* **1972**, *17*, 391–566.

[21] A. Werner, *Chem. Ber.* **1912**, *45*, 3061–3070.

[22] E. L. Muetterties, R. A. Schunn, *Quart. Rev.* **1966**, *20*, 245–299.

[23] Our choice of the three polytopal forms (SQP, TBP_{eq}, and TBP_{ax}) was based on a careful and comprehensive consideration of known pentacoordinate structures and preliminary MM studies. In this way, for example, an SQP with unidentate (py) in the basal plane, which was recently postulated by S. Alvarez, M. Llunell, *J. Chem. Soc. Dalton Trans.* **2000**, 3288–3303, was excluded on the basis of MM criterion, and the fact that it appeared as a transition-state geometry in the $TBP_{eq} \rightleftarrows TBP_{ax}$ interconversion.